Electronic Supplementary Material (ESI) for New Journal of Chemistry.

Supporting Information

Simultaneous gas expansion and nitrogen doping strategy to prepare licorice root residues-derived nitrogen doped porous carbon for supercapacitor

Jiande Gao[a*], Dongying Fan[b], Xiong Liu[a]

[a]*College of Pharmacy, Gansu University of Traditional Chinese Medicine, Research Center of Traditional Chinese Medicine Pharmaceutical Technology and Engineering of Gansu Province Lanzhou 730000, China.*

[b]*Gansu Provincial Hospital of TCM, Lanzhou 730050, China.*

*Corresponding authors: E-mail address: 329315749@qq.com.

S1. Material characterization

X-ray diffraction (XRD) of materials were performed on a diffractometer (D/Max-2400, Rigaku) advance instrument using Cu Kα radiation (k =1.5418 Å). The morphology and microstructure of the materials were tested by field emission scanning electron microscopy (FE-SEM, Carl Zeiss-Ultra Plus, Germany) and transmission electron microscopy (TEM, FEI Tecnai G^2 F20, USA). The Brunauer-Emmett-Teller (BET) surface area of the samples was analyzed by nitrogen adsorption-desorption in a surface area and porosimetry analyzer (ASAP 2020, Micromeritics, U.S.A.). Raman spectra were performed on an inVia Raman spectrometer (Rainie Salt Public Co. Ltd., Britain) with a laser wavelength of 514 nm. The wetting property of carbon materials were analyzed and captured by a high speed camera, Photron FASTCAM Mini UX100 (Photron USA, Inc.).

S2. Electrochemical measurements

The electrochemical properties of the samples were investigated by cyclic voltammetry (CV) and galvanostatic charge/discharge measurements in three-electrode cell and two-electrode configuration using a CHI660E electrochemical workstation (Shanghai Chenghua, China). The cycle-life stability was performed using computer controlled cycling equipment (LAND CT2001A, Wuhan China). Electrochemical impedance spectroscopy (EIS) measurements were performed at the frequency ranging from 0.1 Hz to 100k Hz and an impedance amplitude of ±5 mV at open circuit potential.

The gravimetric capacitance from galvanostatic charge/discharge was calculated by using the formula of $C=I\Delta t/(m\Delta V)$ for the three-electrode system, where I is the charge/discharge current (A) and m is the mass (g) of electrode material, Δt is the discharge time and ΔV is the voltage of the discharge process.

The specific energy density (E, Wh kg^{-1}) and power density (P, W kg^{-1}) for a supercapacitor device can be calculated using the following equations: $E=1/2CV^2$ and $P=E/t$, where C is the specific capacitance of supercapacitor device, V is voltage of discharge process after IR drop in V-t curve, and *t* is the discharge times.

The working electrode was prepared by mixing the carbon active material, super P and polyvinylidene fluoride (PVDF) in a mass ratio of 8:1:1 in N-methyl-2-pyrrolidone (NMP) solution to forms homogeneous slurry. The slurry was pressed onto nickel foam with a working area of 1.0 and dried at 100 ^{o}C for 12 h. The total mass loading of the electrode materials about 4 mg/cm^2. For a supercapacitor device, it should be selected two electrodes with close weights and assembled into the sandwich-type cells device symmetrically by using the thin filter paper and 1 mol L^{-1} Li_2SO_4 solution as the separator and electrolyte, respectively.

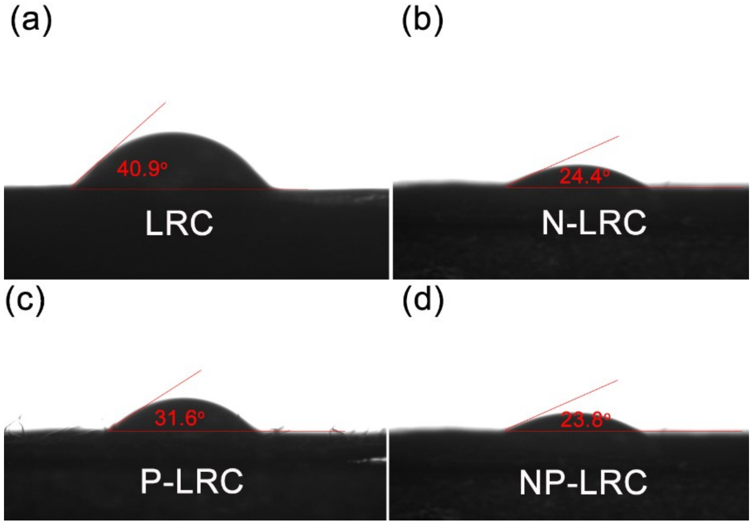

Figure S1. The wettability test of (a) LRC, (b) N-LRC, (c) P-LRC and (d) NP-LRC.

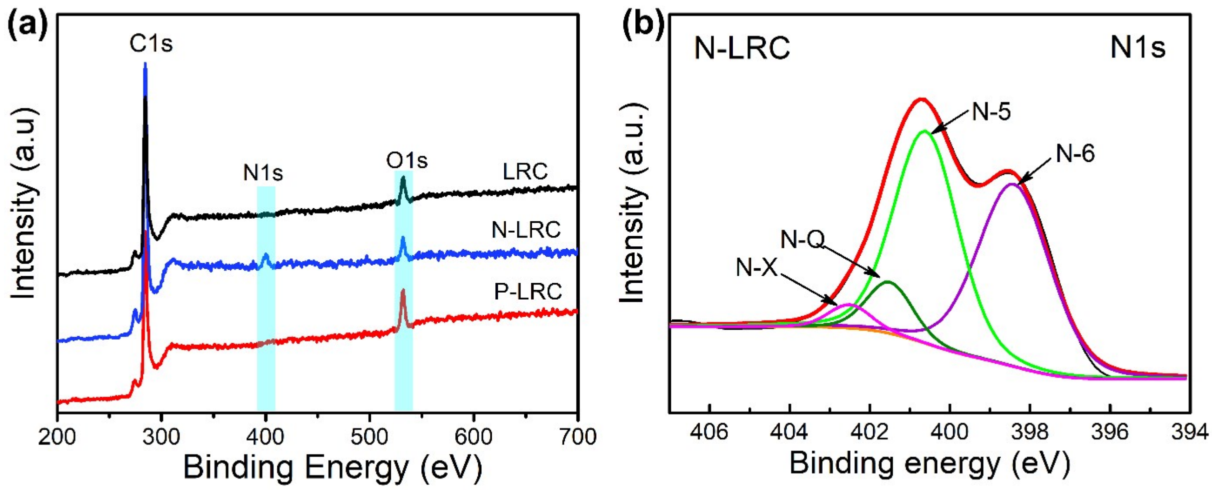

Figure S2. (a) XPS spectrum of LRC, N-LRC and P-LRC materials, (b) high-resolution N1s spectrum of N-LRC.

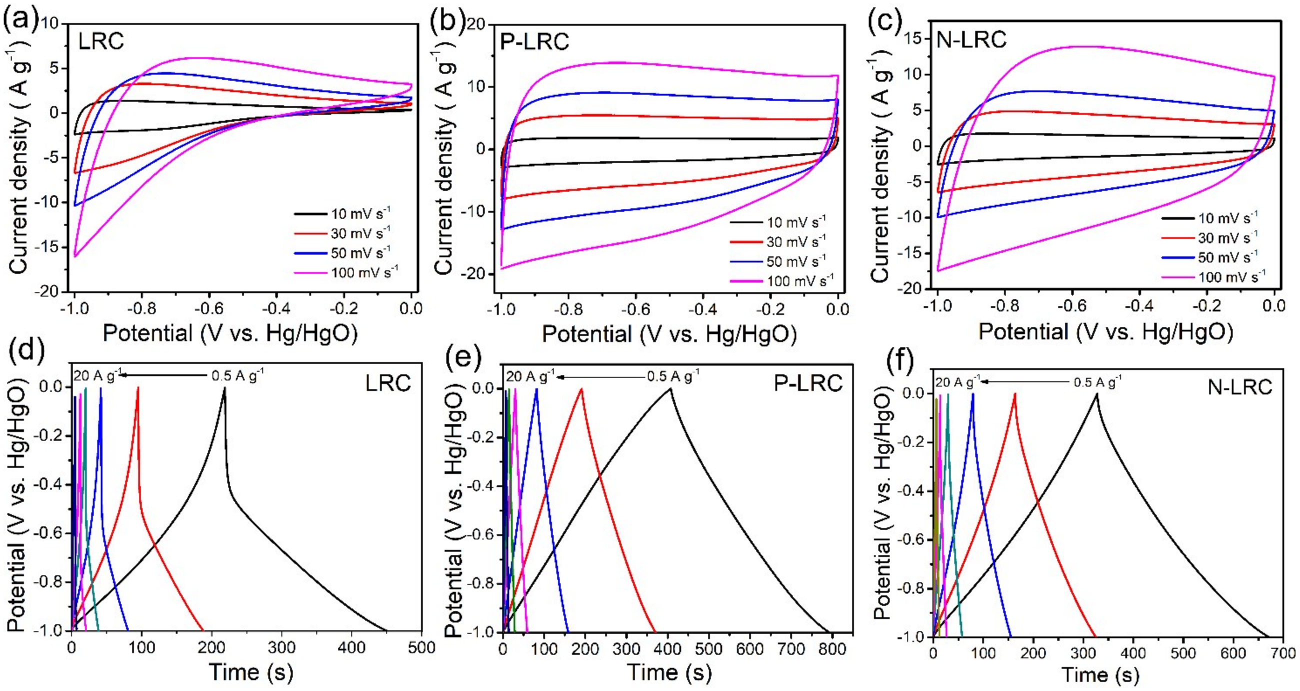

Figure S3. (a-c) CV curves of the LRC, P-LRC and N-LRC materials at various scan rates, (d-f) GCD curves of the LRC, P-LRC and N-LRC materials at various current densities.

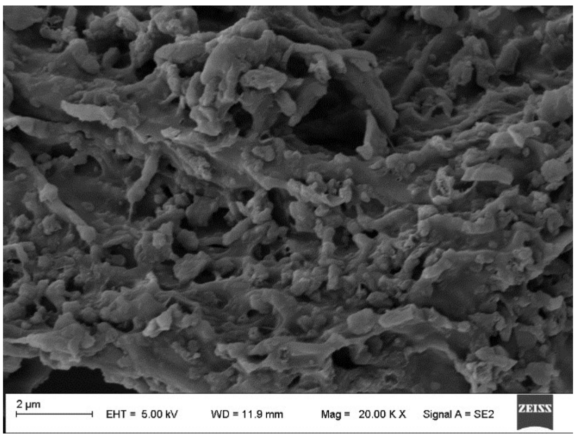

Figure S4. SEM image of the NP-LRC electrode after the cycle stability test.

Table S1. Elemental analysis, BET surface area, and pore structure characterization parameters of carbon materials.

Carbon materials	Elemental analysis			S_{BET}[a] (m^2 g^{-1})	D[b] (nm)	V_{total}[c] (cm^3 g^{-1})
	C%	N%	H%			
LRC	76.43	-	1.31	392.9	3.2	0.18
P-LRC	81.21	-	1.44	1016.8	2.7	0.79
N-LRC	79.46	4.12	1.34	764.3	2.3	0.56
NP-LRC	82.87	4.09	1.29	1257.8	2.2	0.91

[a]Specific surface area determined according to the BET (Brunauer-Emmett-Teller) method.
[b] Adsorption average pore diameter.
[c]Total pore volume.

Table 2. The capacitance values and BET surface area of NP-LRC materials and the carbon electrode materials recently reported in literatures.

Electrode materials	BET surface area (m^2 g^{-1})	Electrolyte	Specific capacitance (current density)	Refs.
peanut shells-based carbon (FE/MG-AC-800)	1427.81	1 M Na_2SO_4	247.28 F g^{-1} (1 A g^{-1})	[S1]
wheat straw-based carbon (PBC)	2115	3 M KOH	294 F g^{-1} (1 A g^{-1})	[S2]
Zanthoxylum Leaves-based carbon	1242.7	2 M KOH	196 F g^{-1} (0.5 A g^{-1})	[S3]
Black locust seed dregs-based carbon (BDPC)	2010.1	6 M KOH	333 F g^{-1} (1 A g^{-1})	[S4]
European deciduous trees-based carbon	614	1 M H_2SO_4	24 F g^{-1} (0.25 A g^{-1})	[S5]
Green-tea wastes-based carbon	1057.8	1 M H_2SO_4	162 F g^{-1} (0.5 A g^{-1})	[S6]
Wood powders-based carbon	868.8	6 M KOH	150.1 F g^{-1} (0.2 A g^{-1})	[S7]
Quinoa-based carbon	2597	6 M KOH	330 F g^{-1} (1 A g^{-1})	[S8]
NP-LRC	1257.8	6 M KOH	221 F g^{-1} (0.5 A g^{-1})	This work

Table S3 Performances comparison of aqueous symmetric supercapacitors used various carbon materials in the references.

Carbon type	Electrolyte	Operation voltage (V)	*E* (Wh kg^{-1})	*P* (W kg^{-1})	Refs.
Licorice root residues-derived nitrogen doped porous carbon (NR-LRC)	Li_2SO_4 (1 M)	1.8	11.7	450	This work
Carbon material (CL-700)	KOH (6 M)	1.0	7.1	124.9	S9
Graphene quantum dots (GQDs)	KOH (6 M)	1.0	9.21	247.75	S10
Porous-hollow carbon nanofibers (HCF800)	KOH (6 M)	1.2	12.99	12 K	S11
CNTAC	TEABF4/PC (1 M)	2.5	12.9	100	S12
Hierarchical porous N, O, S-enriched carbon foam (KNOSC)	Na_2SO_4 (1 M)	1.8	15.2	36K	S13
N, S co-doped porous carbon fibers film (PCFF)	KOH (6 M)	1.0	16.35	147.15	S14
3D hierarchical porous carbon (GHC-17)	KOH (6 M)	1.0	14.65	27.3K	S15
N-containing hierarchical porous carbon spheres (HPCSs)	KOH (7 M)	1.0	7.8	6.2K	S16
N/S co-doped porous carbon nanobowls	KOH (6 M)	1.0	9.6	25	S17
Hierarchical porous carbons (HPCs)	NaCl (1 M)	1.5	15.2	751	S18
Nitrogen-rich porous graphene-like carbon sheets (NPGCs)	KOH (6 M)	1.0	6.53	28.4K	S19
Porous carbon of cicada slough (PCCS)	KOH (6 M)	1.0	9.0CL	227	S20

References

[S1] Guo, F.; Jiang, X.; Jia, X.; Liang, S.; Qian, L.; Rao, Z. Synthesis of biomass carbon electrode materials by bimetallic activation for the application in supercapacitors, *J. Electroanal. Chem.* **2019**, 844, 105-115.

[S2] Du, W.; Zhang, Z.; Du, L.; Fan X.; Shen Z.; Ren, X.; Zhao, Y.; Wei, C.; Wei, S. Designing synthesis of porous biomass carbon from wheat straw and the functionalizing application in flexible, all-solid-state supercapacitors, *J. Alloy. Compd.* **2019**, 797, 1031-1040.

[S3] Xu, Y.; Lei, H.; Qi, S.; Ren, F.; Peng, H.; Wang, F.; Li, L.; Ma, G. Three-dimensional zanthoxylum Leaves-Derived nitrogen-Doped porous carbon frameworks for aqueous supercapacitor with high specific energy, *J. Energy Storage* **2020**, 32, 101970

[S4] Hou, L.; Hu, Z.; Wang, X.; Qiang, L.; Zhou, Y.; Lv, L.; Li, S. Hierarchically porous and heteroatom self-doped graphitic biomass carbon for supercapacitors, Journal of Colloid and Interface Science, 2019, 540, 88-96.

[S5] Jain, A.; Ghosh, M.; Krajewski, M.; Kurungot, S.; Michalska, M. Biomass-derived activated carbon material from native European deciduous trees as an inexpensive and sustainable energy material for supercapacitor application, *J. Energy Storage* **2021**, 34, 102178.

[S6] Sankar, S.; Ahmed, A.T.A.; Inamdar, A.I.; Im, H.; Im, Y.B.; Lee, Y. Kim, D.Y.; Lee, S. Biomass-derived ultrathin mesoporous graphitic carbon nanoflakes as stable electrode material for high-performance supercapacitors, *Mater. Design* **2019**, 169, 107688.

[S7] Wang, C.; Wang, H.; Dang, B.; Wang, Z.; Shen, X.; Li, C.; Sun, Q. Ultrahigh yield of nitrogen doped porous carbon from biomass waste for supercapacitor, *Renewable Energy* **2020**, 156, 370-376.

[S8] Sun, Y.; Xue, J.; Dong, S.; Zhang, Y.; An, Y.; Ding, B.; Zhang, T.; Dou, H.; Zhang, X. Biomass-derived porous carbon electrodes for high-performance supercapacitors, *J. Mater. Sci.* **2020**, 55, 5166-5176.

[S9] Liu, Z. L.; Tian, D.; Shen, F.; Nnanna, P. C.; Hu, J. G.; Zeng, Y. M.; Yang, G.; He, J. S.; Deng, S. H. Valorization of composting leachate for preparing carbon material to achieve high electrochemical performances for supercapacitor electrode. *J. Power Sources* **2020**, *458*, 228057.

[S10] Tian, W. H.; Zhu, J. Y.; Dong, Y.; Zhao, J.; Li, J.; Guo, N. N.; Lin, H.; Zhang, S.; Jia, D. Z. Micelle-induced assembly of graphene quantum dots into conductive porous carbon for high rate supercapacitor electrodes at high mass loadings. *Carbon* **2020**, *161*, 89-96.

[S11] Liu, Y. W.; Liu, Q.; Wang, L.; Yang, X. F.; Yang, W. Y.; Zheng, J. J.; Hou, H. L. Advanced supercapacitors based on porous hollow carbon nanofiber electrodes with high specific capacitance and large energy density.

ACS Appl. Mater. Interfaces **2020**, *12*, 4777-4786.

[S12] Han, J.; Chae, J. S.; Kim, J. C.; Roh, K. C. Facile preparation of composite electrodes for supercapacitors by CNT entrapment into carbon matrix derived from pitch at a softening point. *Carbon* **2020**, *163*, 402-407.

[S13] Peng, H. R.; Yao, B.; Wei, X. J.; Liu, T. Y.; Kou, T. Y.; Xiao, P.; Zhang, Y. H.; Li Y. Pore and heteroatom engineered carbon foams for supercapacitors. *Adv. Energy Mater.* **2019**, *9*, 1803665.

[S14] Chen, L.; Wen, Z. Y.; Chen, L. N.; Wang, W. P.; Ai, Q.; Hou, G. M.; Li, Y. H.; Lou, J.; Ci, L. J. Nitrogen and sulfur co-doped porous carbon fibers film for flexible symmetric all-solid-state supercapacitors. *J. Power Sources* **2020**, *158*, 456-464.

[S15] Zhang, Q.; Han, K.; Li, S.; Li, M.; Li, J.; Ren, K. Synthesis of garlic skin-derived 3D hierarchical porous carbon for high-performance supercapacitors. *Nanoscale* **2018**, *10*, 2427-2437.

[S16] Pang, J.; Zhang, W.; Zhang, H.; Zhang, J.; Zhang, H.; Cao, G.; Han, M.; Yang, Y. Sustainable nitrogen-containing hierarchical porous carbon spheres derived from sodium lignosulfonate for high-performance supercapacitors. *Carbon* **2018**, *132*, 280-293.

[S17] Wang, J.; Liu, H.; Zhang, X.; Shao, M.; Wei, B. Elaborate construction of N/S-co-doped carbon nanobowls for ultrahigh-power supercapacitors. *J. Mater. Chem. A* **2018**, *6*, 17653-17661.

[S18] Wang, C.; Wang, X. F.; Lu, H.; Li, H. L.; Zhao, X. S. Cellulose-derived hierarchical porous carbon for high-performance flexible supercapacitors. *Carbon* **2018**, *140*, 139-147.

[S19] Yang, W.; Hou, L. Q.; Xu, X. W.; Li, Z. H.; Ma, X. L.; Yang, F.; Li, Y. F. Carbon nitride template-directed fabrication of nitrogen-rich porous graphene-like carbon for high performance supercapacitors. *Carbon* **2018**, *130*, 325-332.

[S20] Jia, H. Y.; Sun, J. W.; Xie, X.; Yin, K. B.; Sun, L. T. Cicada slough-derived heteroatom incorporated porous carbon for supercapacitor: Ultra-high gravimetric capacitance. *Carbon* **2018**, *143*, 309-317.